

# Atomistic Theory of Coherent Spin Transfer between Molecularly Bridged Quantum Dots

Joshua Schrier and K. Birgitta Whaley

*Department of Chemistry and Pitzer Center for Theoretical Chemistry, University of California, Berkeley, CA 94720*

Time-resolved Faraday rotation experiments have demonstrated coherent transfer of electron spin between CdSe colloidal quantum dots coupled by conjugated molecules. We employ here a Green's function approach, using semi-empirical tight-binding to treat the nanocrystal Hamiltonian and Extended Hückel theory to treat the linking molecule Hamiltonian, to obtain the coherent transfer probabilities from atomistic calculations, without the introduction of any new parameters. Calculations on 1,4-dithiolbenzene and 1,4-dithiolcyclohexane linked nanocrystals agree qualitatively with experiment and provide support for a previous transfer Hamiltonian model. We find a striking dependence on the transfer probabilities as a function of nanocrystal surface site attachment and linking molecule conformation. Additionally, we predict quantum interference effects in the coherent transfer probabilities for 2,7-dithionaphthalene and 2,6-dithionaphthalene linking molecules. We suggest possible experiments based on these results that would test the coherent, through-molecule transfer mechanism.

## I. INTRODUCTION

Colloidal semiconductor nanocrystals have attracted attention not only because of their size tunable optical properties, but also because of the long-lived spin coherences resulting from full three-dimensional confinement.[1] Potential spintronic and quantum computational applications[2, 3] have led to the development of optical techniques such as time-resolved Faraday rotation (TRFR) for the measurement and manipulation of single spins in these systems,[4, 5, 6] as well as to theoretical methods to describe these properties.[6, 7, 8, 9] With the spin properties of isolated nanocrystals reasonably well understood, attention has now turned to the study of spin in linked nanocrystals. Ouyang and Awschalom observed coherent transfer between 3.4 nm and 7.0 nm diameter colloidal CdSe coupled by 1,4-dithiolbenzene.[10] Electron spin polarization created by optical pumping of the larger nanocrystal is transferred “instantaneously” (within the experimental limitations) and coherently to the smaller nanocrystal. This transfer from lower band gap to larger band gap nanocrystal is evidence against Förster-like transfer mechanisms.[11] Ouyang and Awschalom conclude from their TRFR measurements transfer efficiencies of  $\sim 10\%$  at  $T < 50\text{K}$  and of  $\sim 20\%$  at  $75 \leq T \leq 250\text{K}$ , and attribute this temperature dependence to changes in the conformation of the linking molecules.

Meier *et al.* have developed a transfer Hamiltonian theory describing the TRFR signal as a function of a spin transfer probability and Heisenberg spin-exchange between the coupled nanocrystals.[12] They draw the important conclusion that the TRFR signal at a given probe frequency does not provide enough information to determine the spin transfer probability, and thus the increase in Faraday rotational signal observed experimentally—and interpreted as an increase in spin transfer efficiency for higher temperatures—may also result from increases in the incoherent transfer paths. In this paper, we describe a method for the atomistic description of the coherent spin transfer probability, that uses a semiempirical tight-binding theory for the treatment of the nanocrystals and Extended Hückel theory for the linking molecule. This microscopic approach allows us to calculate the coherent spin transfer for new classes of linking molecules, as well as to study the effects of their molecular conformation in a systematic fashion. Additionally, we explore the variability of the spin transfer due to the distribution of surface sites of the nanocrystal, which is a previously unrecognized factor in the construction of devices based on this system.

## II. THEORY

### A. Semiempirical Hamiltonian Calculation

To treat the CdSe nanocrystals, we have used the orthogonal nearest-neighbor  $sp^3s^*$  basis tight-binding (TB) approach, using the standard semiempirical matrix elements,[13] transformed from zinc blende to hexagonal crystal structure.[14]. These parameters have been shown previously to reproduce the optical[15] and magneto-optical[8] properties of this system. The surface sites of the nanocrystal are passivated with oxygen-like ligands to mimic the TOPO ligands used experimentally.

Since the TB parameterization does not extend to carbon or hydrogen atoms, we have treated the linking molecules using Extended Hückel theory (EHT).[16, 17] As in the TB method used for the nanocrystal, EHT uses a basis of valence Slater orbitals. Following Ref. 14, where the ionization energy of the cation was used to determine a consistent

energy scale for the CdS and CdSe TB parameterizations in order to produce a parameterization for CdS<sub>x</sub>Se<sub>1-x</sub>, we require the ionization energies (diagonal TB Hamiltonian terms) of the S and Se atoms to be consistent between the TB and EHT schemes. This leads to a global shift of the EHT Hamiltonian energies by 11.155 eV to make it consistent with the TB energy scale. The insensitivity of our results to the exact value of this shift is demonstrated in Section III A 2. An  $sp^3$  Slater-orbital basis is used for the non-Cd atoms (H, C, S), using the parameters of Ref. 18, and the  $sp^3s^*$  Slater-orbital basis of Ref. 19 is used for the Cd atoms. These calculations are performed using a modified version of the Yaehmop program.[18] For simplicity, and for better comparison with the work of Meier *et al.*, [12] we have neglected the spin-orbit coupling of the linking molecule. This may be justified by noting that the spin-orbit coupling constants for carbon and hydrogen atoms are small.[20] Nonetheless, this could be included in future studies.[21, 22] Additionally, our treatment considers only small applied magnetic fields, such that Zeeman splitting of the nanocrystal and molecule levels is small.

There are several possible alternatives to the present TB/EHT Hamiltonian treatment that may be useful for future research on other molecularly linked nanocrystal systems. For silicon nanocrystals linked by hydrocarbon molecules, one could use the orthogonal nearest-neighbor tight-binding parameterizations developed for Si-C alloys.[23] For metal nanocrystals, one might use the non-orthogonal tight binding method of Papaconstantopolous and coworkers,[24, 25] combined with either EHT[16] or a Harrison tight-binding parameterization[26] for the linking molecule. Additionally, one might use other semiempirical techniques from quantum chemistry, such as INDO/S.[27, 28]

## B. Determination of the Nanocrystal Surface Local Density of States

The transfer probability calculation, described below, requires the use of the local density of states (LDOS) for the molecular contact sites. Unlike in typical molecular electronics calculations, e.g., Ref. 29, in which the final contact is taken to be part of a bulk lead and consequently the bulk DOS at the Fermi energy may be used, in our case the LDOS will be a function of the nanocrystal surface site connected to the linking molecule, and must be calculated explicitly. By calculating the Green's function,  $G_{NC}(E)$ , of the nanocrystal Hamiltonian,  $H_{NC}$ ,

$$G_{NC}(E) = [(E + i\eta)I - H_{NC}]^{-1} \quad (1)$$

(where  $i = \sqrt{-1}$  and  $\eta$  is infinitesimal), the LDOS,  $\rho_{NC}(E, j)$ , for the basis orbital  $j$  is given simply by

$$\rho_{NC}(E, j) = -\pi^{-1} \text{Im} \left[ G_{NC}(E)_{jj} \right], \quad (2)$$

or alternatively by

$$g_{NC}(E, j) = \text{Im} \left[ G_{NC}(E)_{jj} \right]. \quad (3)$$

According to previous experimental[30, 31, 32, 33, 34] and theoretical[14] work, group VI elements (such as S and O) bond preferentially to the Cd atom surface sites on the nanocrystal. Consequently, this calculation is made for each of the  $sp^3s^*$  Cd basis orbitals on the 84 surface Cd sites of the 3.4 nm diameter nanocrystal, and for each of the  $sp^3s^*$  Cd basis orbitals on the 243 surface Cd sites of the 5.0 nm diameter nanocrystal, over energy intervals of  $\Delta E = 0.01$  eV. We use the same nanocrystal structures as in our previous work.[8] This stage of the calculation is time consuming, since determining  $G(E)$  requires a matrix inversion for each value of E considered. However the results for a given nanocrystal are independent of the linking molecule, and thus need only be determined once and stored for future use. We also note that this process adds artificial peaks in the band-gap region for the  $T(E)$  plots, which are due to surface states induced by the removal of the ligands for the calculation of  $G(E)$ .

## C. Transfer Probability Calculation

Following the treatment of Datta,[35] we may express the Green's function for the entire system as

$$G_{sys}(E, j, k) = [EI - H_{mol} - \Sigma_{NC1}^R(E, j) - \Sigma_{NC2}^R(E, k)]^{-1}, \quad (4)$$

where the self energy for a given nanocrystal surface site atomic orbital (AO)  $j$ , is given by

$$\Sigma_{NC1}(E, j) = \tau_{NC1}^\dagger(j)g_{NC1}(E, j)\tau_{NC1}(j). \quad (5)$$

Here  $\tau(j)$  is the portion of the Hamiltonian matrix between the nanocrystal surface site AO  $j$  and the linking molecule basis functions. These matrix elements are determined from the EHT calculation by including two Cd atoms, given with a TB/EHT consistent  $sp^3s^*$  Slater orbital basis as described in Section II A. Defining

$$\Gamma_{NC1}(E, j) = i \left[ \Sigma_{NC1}(E, j) - \Sigma_{NC1}^\dagger(E, j) \right], \quad (6)$$

the transmission probability is obtained as

$$T(E, j, k) = \text{Tr} \left[ \Gamma_{NC1}(E, j)G_{sys}(E, j, k)\Gamma_{NC2}(E, k)G_{sys}^\dagger(E, j, k) \right]. \quad (7)$$

The transmission function is calculated for each of the possible  $j, k$  combinations, at energy intervals of  $\Delta E = 0.01$  eV. This is then processed to determine the statistics of  $T(E)$  as a function of the surface-site connections. Our treatment assumes that the transfer process is entirely coherent, and as a result may overestimate the observed transfer probability due to neglect of incoherent loss channels.

### III. RESULTS

#### A. 1,4-dithiolbenzene

##### 1. Surface Site Dependence

The 1,4-dithiolbenzene molecule, shown in Figure 1a, consists of a benzene ring with sulfur atoms attached to opposite ends of the ring, and is commonly used in molecular conduction studies.[29, 36] To begin our study, we took the MM2[37] molecular-dynamics optimized structure of 1,4-dithiolbenzene, and replaced the thiol hydrogen atoms with Cd atoms at the appropriate bond length (2.63 Å)[26], as depicted in Figure 2. In Figure 2 the solid and dashed lines indicate the average and median values of  $T(E)$ , respectively. The mean, median and standard deviation of  $T(E)$  are taken over all of the  $243 \times 84 = 20412$  possible connections of the 1,4-dithiolbenzene molecule between surface sites of the two nanocrystals. Each calculation was taken over the -1 to 6 eV energy range, at intervals of  $\Delta E = 0.01$  eV. In the region of -0.7 to 0 eV, the mean  $T(E)$  oscillates between values of approximately 0.13 and 0.06; the median  $T(E)$  in this region oscillates between 0.06 and 0.04. In the region of 2.4 to 3 eV, both the mean and the median  $T(E)$  reach a peak at 2.6 eV, of value 0.30 and 0.21, respectively. Prior to this peak, the mean  $T(E)$  ranges from 0.04 to 0.18 in the region of 2.4 to 2.6 eV, and from 0.10 to 0.08 in the region from 2.6 to 3 eV; the median  $T(E)$  follows the same qualitative behavior, but with lower values. The mean transmission probabilities in both of these energy ranges, corresponding to the hole and electron transmission probabilities, are similar to those determined by Meier *et al.* from their analysis of the TRFR data.[12] Note that the latter was non-microscopic and employed a fit to the experimental results.

##### 2. Role of the Energy Scale Shift

As mentioned in Section II A, the absolute energy scales of the TB and EHT Hamiltonians are not the same, requiring an energy shift to make them consistent. By calculating the average difference between the S and Se atomic orbital ionization potentials (diagonal Hamiltonian matrix elements) obtained in the two different methods, one obtains an average shift of 11.155 eV. To explore the dependence of our results on the exact value of this energy correction, we performed calculations for  $T(E)$  using shift corrections in the range of 10.0 to 12.0 eV, at intervals of 0.5 eV, using the same molecular geometry as in the previous section. We found that the changes in mean  $T(E)$  due to the different choices of energy shift lie within the variation due to surface site attachment for calculations made with a shift of 11.155 eV, with the exception of some peaks in the nanocrystal band gap region and in the region below -0.75 eV (in the TB parameterization, 0 eV corresponds to the highest occupied molecular orbital). These results indicate that the exact value of this shift is unimportant for band edge electrons and holes, compared to the effects of variation due to the surface site attachment of the molecule.

### 3. Conformational Dependence

Previous theoretical studies of thiolated molecules between gold contacts by Kornilovitch and Bratkovsky indicate a strong dependence of the transmission function on the conformation of the molecule, due to the directionality of the  $p$ -type atomic orbital interactions between molecule and contact atoms.[29, 36] This conformational dependence was conjectured by Ouyang and Awschalom to be responsible for the temperature dependence of the spin transfer observed in the experimental study.[10] This is straightforward to study within the current microscopic theory. We first examined the case in which both of C-S and S-Cd bonds are collinear in the plane of the benzene ring, shown in Figure 3. Such conformation shows a decrease in both the hole and electron region  $T(E)$  values below  $\sim 0.05$ . Next we examined the effects of moving the S-Cd bond in the plane and out of the plane of the benzene ring, shown respectively in Figures 4 and 5. For the in-plane motions, the value of  $T(E)$  below 2.5 eV remains relatively constant, and the region between 4-5 eV shows the greatest changes. When one of the Cd-S bonds was approximately collinear with the S-C bond, the effect due to moving the other bond was negligible compared to the case of both Cd-S collinear with their respective S-C bonds. Bends of both C-S-Cd linkages were required to obtain an enhancement in  $T(E)$ . For the out of benzene plane motions, shown in Figure 5, we found enhancements in  $T(E)$  in the range of -1 to +0.5 eV, with changes in the 4 to 5 eV range only for the extreme angles. As seen in the figure, the  $T(E)$  for the hole reached a maximum of  $\sim 0.25$ . We note that the transmission probability for the hole is dependent on the out of plane component of the C-S-Cd dihedral angle, while the electron transmission probability is dependent on the in-plane angle.

#### B. 1,4-dithiolcyclohexane

As shown in Figure 1b, 1,4-dithiolcyclohexane differs from dithiolbenzene by the absence of pi-bonding between carbon atoms in the ring (due to bonding with additional hydrogen atoms making it a saturated molecule), which in turn decreases its conductivity. Just as for the 1,4-dithiolbenzene discussed in Section III A 1, we began with the MM2 optimized structure for 1,4-dithiolcyclohexane. The results for this initial conformation (the so-called “boat” conformation[38] of cyclohexane) are shown in Figure 6. In the region of -1 to 0 eV and 2 to 3 eV we found the mean  $T(E)$  to be less than 0.01, with the exception of peaks at 2.6 eV and 2.8 eV, where  $T(E)$  rises to  $\sim 0.04$ . We then performed all of the C-S-Cd rotations that were carried out in Section III A 3 for 1,4-dithiolbenzene. The mean  $T(E)$  determined in each of these calculations is plotted as a separate line in Figure 7. From this it is evident that  $T(E)$  for this saturated linking molecule is insensitive to conformational changes in the valence and conduction band edge energy regions, remaining near zero for all cases. This is consistent with the experimental results reported by Ouyang and Awschalom.[10] The comparison to 1,4-dithiolcyclobenzene is discussed in detail in Section IV B.

#### C. 2,6-dithiolnaphthalene

Dithiolnaphthalene consists of two aromatic rings joined at an edge. We considered two placements of the thiol groups on this ring structure in order to investigate the effect of length of the aromatic linker and the possibility of quantum interference effects. The first placement corresponds to 2,6-dithiolnaphthalene, shown in Figure 1c. The ring structure was MM2 optimized, and the C-S-Cd conformation was set to the maximal  $T(E)$  conformation determined in Section III A 3 for 1,4-dithiolbenzene. Due to the higher computational costs as a result of the larger molecule size, we examined only the cases depicted in the cartoon in Figure 8, in which both C-S-Cd dihedral angles with respect to the plane of the naphthalene ring were oriented in the same direction and in the opposite direction (denoted “up, up” and “up, down”, respectively), and the case of the C-S-Cd angle in the plane of the ring (denoted “flat”). As shown in Figure 8,  $T(E)$  in the regions of -1 to 0 eV and 2.0 to 3.5 eV are near zero for all of the conformations we examined. In the energy range between 4 to 5 eV, the bent conformation with both C-S-Cd units oriented in the same direction was found to have a peak  $T(E)$  of 0.07, as compared to 0.12 for the conformation with the C-S-Cd units in opposite directions.

#### D. 2,7-dithiolnaphthalene

We examined the analogous conformations as described in the previous section for the 2,7-dithiolnaphthalene linked nanocrystals, shown in Figure 1d, and in the cartoons in Figure III D. As shown in Figure 9,  $T(E)$  in the region of -1 to 0 eV varies between 0.09 and 0.02 for the bent conformations, and 0.01 to zero for the flat conformation. In the 2.0 to 4.0 eV range, all mean  $T(E)$  values are near zero. Both conformations have similar mean  $T(E)$  values over the

entire energy range, and unlike the 2,6-dithiolnaphthalene discussed above, the variation in  $T(E)$  due to surface site attachment was also found to be similar for both bent conformations. A detailed analysis of the difference in  $T(E)$  for the two substituted naphthalene molecules is presented in Section IV D below.

## IV. DISCUSSION

### A. Surface Site Dependence

The variations in  $T(E)$  due to the specific surface site attachments, discussed in Section III A 1, and observed in all of the calculations described subsequently, presents a quality-control problem for the construction of individual spin-manipulating devices such as required for quantum computation. While the ensemble of molecularly linked nanocrystals observed in optical experiments will have a non-negligible spin transfer percentage, any particular device may have much better (or much worse) performance. However, there may be chemical effects during the assembly process which preferentially select a subset of surface sites for binding to the molecule. Alternately, use of highly symmetric nanocrystals, such as the icosahedral Si nanocrystals recently predicted by Zhao *et al.*, [39] may also simplify the problem by reducing the number of possible surface sites available for attachment. In any case, we conclude that it is essential to understand the effect of variability in surface site linkage on the coherent spin transfer probability.

### B. Comparison of Theoretical and Experimental Results for 1,4-dithiolbenzene and 1,4-dithiolcyclohexane

The results presented in Section III A with Section III B agree with the measurements of Ouyang and Awschalom (10-20% transfer for dithiolbenzene, no transfer for dithiolcyclohexane) [10] and corresponding estimates by Meier *et al.* (6-13% for dithiolbenzene)[12]. Unlike the latter study, we have neglected the role of the coulomb contribution due to charging of the QDs, and so our computed forward and backware transfer probabilities are equivalent. Furthermore, since the estimate of the transfer probability in Meier *et al.* is derived from a fitting to experimental data, it implicitly performs an average over conformations. As we discuss in the next section, this can lead to changes in the transfer probability. Consequently we can only expect qualitative agreement from calculations for a single conformation. Nevertheless, our calculation of negligible valence and conduction carrier transfer for the dithiolcyclohexane linked region shows the qualitative benefit of the atomistic approach, and suggests that this approach may be useful to provide parameters for model studies in future work.

### C. Conformation as a Mechanism for Temperature Dependence

Our results results for the conformational dependence of  $T(E)$ , shown in Figures 3-5, are consistent with the explanation of temperature dependence of TRFR put forward by Ouyang and Awschalom, [10] namely, that different molecular conformations populated as a function of temperature can exhibit different spin transfer properties. In addition to conformational dependence, thermally populated vibrational modes may play a role in the temperature dependence. We have neglected explicit coupling of the electronic modes to vibrational modes here, although in principle the method may be extended to treat this. [35, 40, 41] We suggest that this may be studied experimentally by means of isotopically-substituted linking molecules. If the temperature dependence is primarily due to the molecular conformation, the isotopic substitutions will have only a small effect on the observed spin transfer. Alternately, if the temperature dependence is due to population of some subset of vibrational states, selectively isotopically substituted linker molecules could then be used to identify which vibrational modes play a dominant role, by making use of isotope effects on vibrational frequencies.

### D. Quantum Interference Effects

Baer and Neuhauser demonstrated that the phase coherence (or anticoherence) through a molecular ring can be used as a molecular XOR switch. [42, 43] In a simple Hückel model at half-filling, the wavefunction changes sign at every second site, giving rise to coherent transfer when the lengths of the two complementary portions of the ring differ by  $2n$  sites, and resulting in “anti-coherent” transfer when the corresponding lengths differ by  $2n + 2$  sites. This effect has also been demonstrated in density-functional calculations of polycyclic hydrocarbon molecules. [44] In Section III C and Section III D we predict that this difference between coherent and anticoherent transfer for different loop lengths should be visible in the substituted naphthalene-linked nanocrystals. In terms of the Hückel model

described above, this can be understood by counting the number of carbon atoms between the thiol groups for the naphthalene molecules shown in Figure 1c and 1d, traversing the upper and lower portions of the ring. For the 2,6-dithiolnaphthalene molecule shown in Figure 1c, there is a difference of two sites for the upper and lower paths, resulting in destructive interference. For the 2,7-dithiolnaphthalene molecule shown in Figure 1d, the lengths of the upper and lower paths between the thiol groups is the same, resulting in constructive interference. This suggests an experimental test of the coherent transport mechanism proposed by Meier *et al.*, [12] that was taken as a given ansatz in this work. Specifically, an observation of significant spin-transfer between 2,7-substituted naphthalene linked nanocrystals without significant transfer for 2,6-substituted naphthalene linked nanocrystals would provide positive evidence that hole conduction occurs through the molecule. Furthermore, we note that extending the distance between the nanocrystals to approximately 12.9 Å as is the case with the naphthalene linker, and finding persistence of substantial spin transfer, would provide further evidence against the possibility of Förster-like [11] spin transfer mechanisms.

## V. SUMMARY

We have developed an atomistic semi-empirical theory for the coherent transfer of carriers between molecularly linked nanocrystals. Our results for 1,4-dithiolbenzene and 1,4-dithiolcyclohexane linked nanocrystals are in qualitative agreement with both experimental [10] and empirical model theoretical [12] work on these systems. Using an atomistic approach, based on a semiempirical tight-binding description of the nanocrystals, and extended Hückel theory description of the linker molecules, and a Green's function formalism for the description of the transfer probability, we examined the role of surface site attachment and linking molecule conformation on the coherent transfer probability. The variation due to the former is a new insight which may be overlooked in ensemble measurements; our calculations indicate a standard deviation in  $T(E)$  due to surface site attachments of 0.1-0.2. The variation due to the latter supports the hypothesis of Ouyang and Awschalom that the temperature dependence of the spin transfer results from conformational changes in the linking molecule. In addition, we have predicted a quantum interference effect in the coherent transfer probabilities for 2,6-dithiolnaphthalene and 2,7-dithiolnaphthalene linked nanocrystals, which we propose be used as an experimental test of the coherent nature of the transfer.

## VI. ACKNOWLEDGEMENTS

J.S. thanks the National Defense Science and Engineering Grant (NDSEG) program and U.S. Army Research Office Contract/Grant No. FDDAAD19-01-1-0612 for financial support. This work was also supported by the Defense Advanced Research Projects Agency (DARPA) and the Office of Naval Research under Grant No. FDN00014-01-1-0826, and the National Science Foundation under Grant EIA-020-1-0826.

- 
- [1] D. D. Awschalom and J. M. Kikkawa, *Physics Today* **52**, 33 (1999).
  - [2] D. Loss and D. P. DiVincenzo, *Phys. Rev. A* **57**, 120 (1998).
  - [3] S. A. Wolf, D. D. Awschalom, R. A. Buhrman, J. M. Daughton, S. von Molnar, M. L. Roukes, A. Y. Chtchelkanova, and D. M. Treger, *Science* **294**, 1488 (2001).
  - [4] J. A. Gupta, D. D. Awschalom, X. Peng, and A. P. Alivisatos, *Phys. Rev. B* **59**, R10421 (1999).
  - [5] J. A. Gupta, Ph.D. thesis, University of California, Santa Barbara (2002).
  - [6] J. A. Gupta, D. D. Awschalom, A. L. Efros, and A. V. Rodina, *Phys. Rev. B* **66**, 125307 (2002).
  - [7] A. V. Rodina, A. L. Efros, M. Rosen, and B. K. Meyer, *Mat. Sci. Eng. C* **19**, 435 (2002).
  - [8] J. Schrier and K. B. Whaley, *Phys. Rev. B* **67**, 235301 (2003).
  - [9] P. Chen and K. B. Whaley, *Phys. Rev. B* **70**, 045311 (2004).
  - [10] M. Ouyang and D. D. Awschalom, *Science* **301**, 1074 (2003).
  - [11] A. O. Govorov, *Phys. Rev. B* **68**, 075315 (2003).
  - [12] F. Meier, V. Cerletti, O. Gywat, D. Loss, and D. D. Awschalom, *Phys. Rev. B* **69**, 195315 (2004).
  - [13] P. E. Lippens and M. Lannoo, *Phys. Rev. B* **41**, 6079 (1990).
  - [14] S. Pokrant and K. B. Whaley, *Eur. Phys. J. D* **6**, 255 (1999).
  - [15] K. Leung, S. Pokrant, and K. B. Whaley, *Phys. Rev. B* **57**, 12291 (1998).
  - [16] R. Hoffmann, *J. Chem. Phys.* **39**, 1397 (1963).
  - [17] M.-H. Whangbo, *Theor. Chem. Acc.* **103**, 252 (2000).
  - [18] G. A. Landrum (1997), yet another extended Hückel molecular orbital package (YAeHMOP). Cornell University Ithara. <http://overlap.chem.cornell.edu:8080/yaehmop.html>.

- [19] N. A. Hill and K. B. Whaley, *Chem. Phys.* **210**, 117 (1996).
- [20] J. R. Morton, J. R. Rowlands, and D. H. Whiffen, *Atomic properties for interpreting ESR data* (1962), National Physical Laboratory – BPR 13.
- [21] T. P. Pareek and P. Bruno, *Phys. Rev. B* **65**, 241305(R) (2002).
- [22] T. P. Pareek and P. Bruno, *Pramana* **58**, 293 (2002).
- [23] J. Robertson, *Phil. Mag. B* **66**, 615 (1992).
- [24] R. E. Cohen, M. J. Mehl, and D. A. Papaconstantopoulos, *Phys. Rev. B* **50**, R14694 (1994).
- [25] M. J. Mehl and D. A. Papaconstantopoulos, *Phys. Rev. B* **54**, 4519 (1996).
- [26] W. A. Harrison, *Electronic Structure and the Properties of Solids* (Dover, 1989).
- [27] J. Ridley and M. Zerner, *Theoret. Chim. Acta* **32**, 111 (1973).
- [28] J. Ridley and M. Zerner, *J. Mol. Spectrosc.* **50**, 457 (1974).
- [29] P. E. Kornilovitch and A. M. Bratkovsky, *Phys. Rev. B* **64**, 195413 (2001).
- [30] L. R. Becerra, C. B. Murray, R. G. Griffin, and M. G. Bawendi, *J. Chem. Phys.* **100**, 3297 (1994).
- [31] G. Rafeletos, S. Nørager, and P. O’Brien, *J. Mater. Chem.* **11**, 2542 (2001).
- [32] J. Taylor, T. Kippeny, and S. J. Rosenthal, *J. Cluster Sci.* **12**, 571 (2001).
- [33] H. Düllefeld, K. Hoppe, J. Kolny, K. Schilling, H. Weller, and A. Eychmüller, *Phys. Chem. Chem. Phys.* **4**, 4747 (2002).
- [34] A. C. Carter, C. E. Bouldin, K. M. Kemmer, M. I. Bell, J. C. Woicik, and S. A. Majetich, *Phys. Rev. B* **55**, 13822 (1997).
- [35] S. Datta, *Electron Transport in Mesoscopic Systems* (Cambridge University Press, Cambridge, 1997).
- [36] P. E. Kornilovitch and A. M. Bratkovsky, *Ann. N.Y. Acad. Sci.* **960**, 193 (2002).
- [37] N. L. Allinger, *J. Am. Chem. Soc.* **99**, 8127 (1977).
- [38] R. T. Morrison, R. N. Boyd, and R. K. Boyd, *Organic Chemistry* (Benjamin Cummings, San Francisco, 1992), sixth ed.
- [39] Y. Zhao, Y.-H. Kim, M.-H. Du, and S. B. Zhang, *Phys. Rev. Lett.* **93**, 015502 (2004).
- [40] Y.-C. Chen, M. Zwolak, and M. D. Ventra, *Nano Lett.* **4**, 1709 (2004).
- [41] M. Čížek, M. Thoss, and W. Domcke, *Phys. Rev. B* **70**, 125406 (2004).
- [42] R. Baer and D. Neuhauser, *J. Am. Chem. Soc.* **124**, 4200 (2002).
- [43] R. Baer and D. Neuhauser, *Chem. Phys.* **281**, 353 (2002).
- [44] D. Walter, D. Neuhauser, and R. Baer, *Chem. Phys.* **299**, 139 (2004).

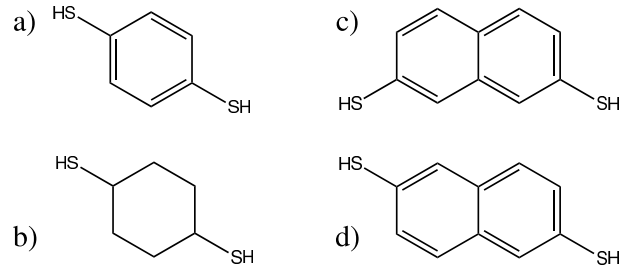


FIG. 1: Linking molecules treated in this study: a) 1,4-dithiolbenzene; b) 1,4-dithiolcyclohexane; c) 2,6-dithiolnaphthalene; d) 2,7-dithiolnaphthalene.

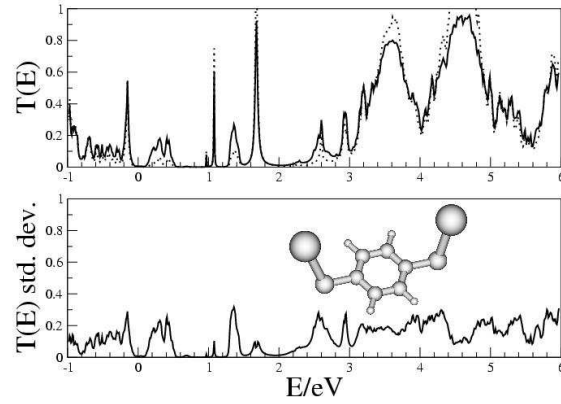


FIG. 2:  $T(E)$  (top) and standard deviation of  $T(E)$  (bottom) for 1,4-dithiolbenzene linked CdSe nanocrystals of 3.4 nm and 5.0 nm diameter. The MM2 optimized conformation of the molecule used in this calculation is shown as the inset cartoon. The black solid and black dashed lines indicate the average and median  $T(E)$ , respectively. The standard deviation of  $T(E)$  results from variations due to the molecule-nanocrystal surface site attachments, as described in Section III A 1. The mean value of  $T(E)$  in the conduction band region (-0.7 - 0 eV) oscillates between 0.06-0.13. Peaks in  $T(E)$  in the bandgap region (0-2.4 eV) results from artificial surface states due to ligand removal in the calculation of  $G(E)$ .

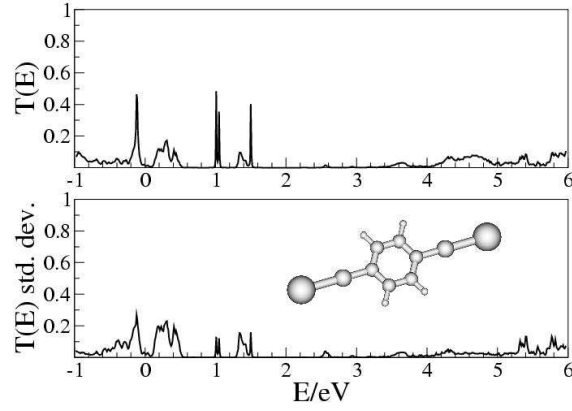


FIG. 3:  $T(E)$  for the flat conformation of the 1,4-dithiolbenzene linker molecule, in which both the C-S and S-Cd bond are collinear in the plane of the benzene ring. The upper figure shows mean  $T(E)$  and the lower figure the standard deviation, due to the variability in surface site attachment. As compared to the reference conformation in Figure 2, the hole energy region transfer probabilities are reduced by half, and the electron energy region  $T(E)$  is nearly zero.

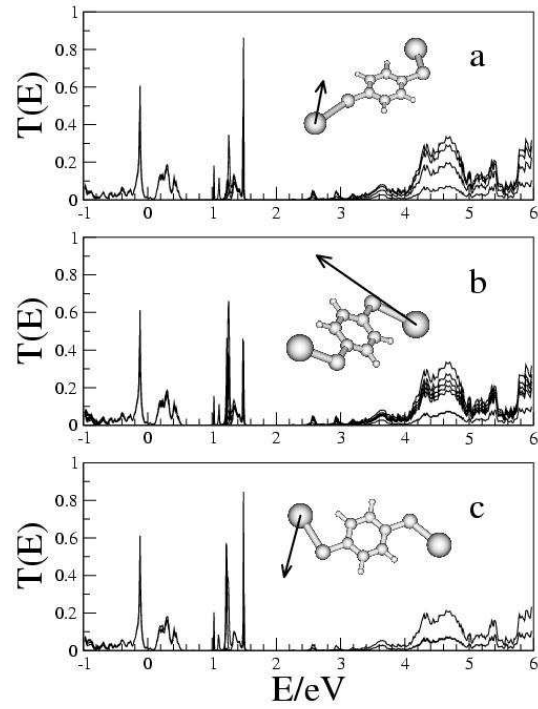


FIG. 4: Effect on  $T(E)$  of in-plane bond angle changes from the flat conformation of 1,4-dithiolbenzene linked nanocrystals. Arrows from the molecule indicate the direction of the motion studied; each line in the plots indicates a different conformation along that direction.

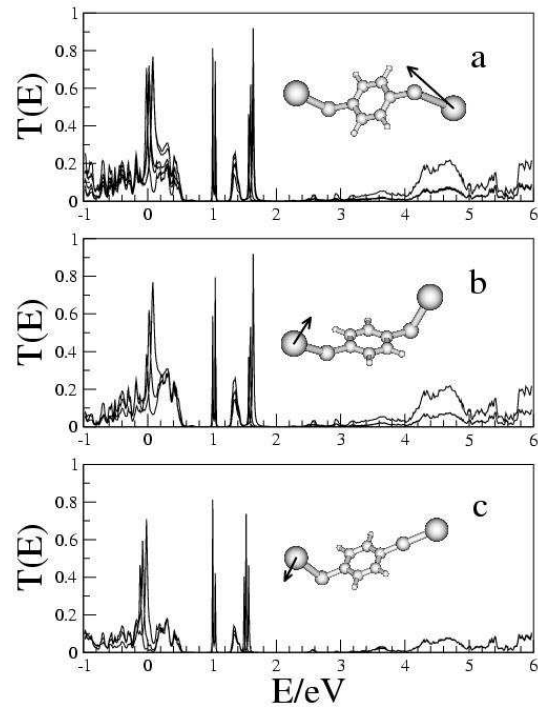


FIG. 5: Effect on  $T(E)$  of out-of-plane bond angle changes from the flat conformation of 1,4-dithiolbenzene linked nanocrystals. Arrows from the molecule indicate the direction of the motion studied; each line in the three plots indicates a different conformation along that direction.

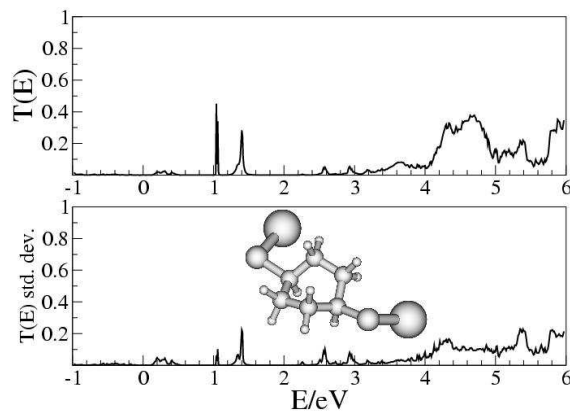


FIG. 6: Mean  $T(E)$  and standard deviation for the MM2-optimized (“boat”) conformation of 1,4-dithiolcyclohexane linked nanocrystals. Note the dramatic decrease in  $T(E)$  over the entire energy range as compared with the conjugated linking molecule 1,4-dithiolbenzene, shown in Figure 2.

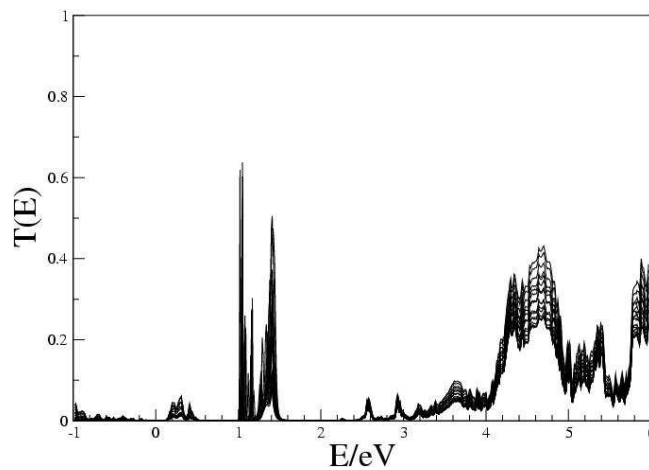


FIG. 7: Effect of C-S and S-Cd bond rotations on the transmission probability,  $T(E)$ , for 1,4-dithiolocyclohexane. The results for each C-S and S-Cd rotation calculated as described in Section III B are shown as individual lines in the figure. No significant changes in  $T(E)$  are observed for any of these rotational motions.

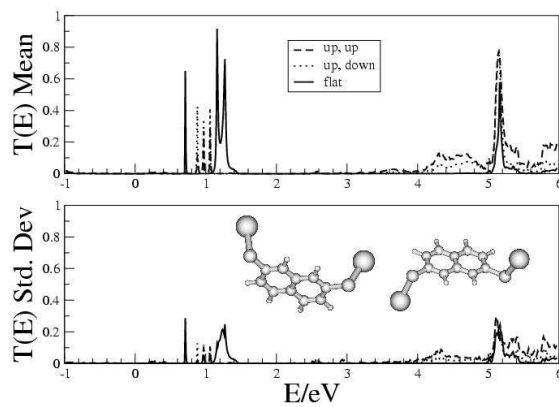


FIG. 8: Mean  $T(E)$  and surface site standard deviation for 2,6-dithiolnaphthalene linked nanocrystals. In the ranges of  $E = -1 \rightarrow 0$  eV and  $E = 2.0 \rightarrow 3.5$  eV,  $T(E)$  was found to be near zero for all three conformations. This results from destructive quantum interference of the electron paths, as discussed in detail in Section IV D.

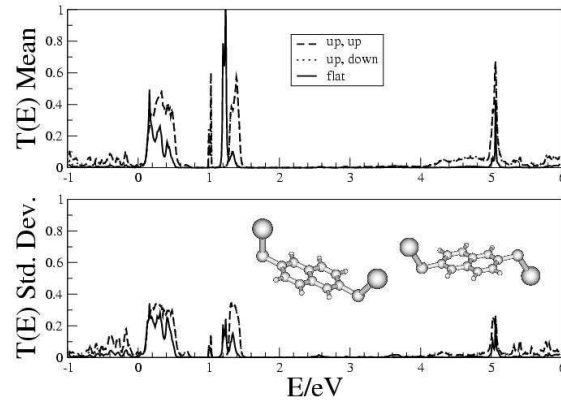


FIG. 9: Mean  $T(E)$  and surface site standard deviation for 2,7-dithiolnaphthalene linked nanocrystals. In contrast to the result for 2,6-dithiolnaphthalene shown in Figure 8, constructive quantum interference of the electron paths causes a non-zero  $T(E)$  of between 0.02 to 0.09 in the region of  $E = -1 \rightarrow 0$ eV that is evident for all three conformations.